

Jana RAUTOVÁ*, Milada KOZUBKOVÁ**

INFLUENCE OF AIR CONTENT IN WATER ON CAVITATION REGION
IN MATHEMATICAL MODEL

VLIV VZDUCHU A VODNÍ PÁRY NA VZNIK KAVITACE PŘI MODELOVÁNÍ

Abstract

The air content in the water is parameter, which plays a big role in formation of cavitation region. This value is not measured in physical experiments. Mathematical models of cavitation take the air content into account. The zero value causes even non- convergent solution. In this paper the air content values in Singhal cavitation model are tested and the influence on the size of cavitation region is evaluated. The results are compared with physical experiment, defined by the water flow through Laval nozzle.

Abstrakt

Obsah vzduchu ve vodě je parametr, který hraje významnou roli při tvorbě kavitačních oblastí. Ve fyzikálních experimentech se jeho hodnota zpravidla neurčuje. Matematické modely kavitace obsah vzduchu také zohledňují. Nulová hodnota způsobuje dokonce nekonvergenci numerického řešení. V článku jsou testovány hodnoty vzduchu v Singhalově modelu kavitace a vyhodnocen jeho vliv na velikost kavitační oblasti. Výsledky jsou konfrontovány s experimentem, který se týká proudění vody Lavalovou dýzou.

1 INTRODUCTION

Problem is focused on fluid flow through Laval nozzle and formation of cavitation region. By the flow through the contracted part of the Laval tube the velocity increases, pressure decreases and cavitation phenomenon is observed. The cavitation region changes the dimension due to increasing fluid flow. This region consists of water, vapour and air, so the flow is defined as multiphase flow. The amount of air in the water was not traced in physical experiment, so this value had to be estimated. Therefore at first the influence of air in water was tested (theoretical case). In the second variant the cavitation model without air was computed and in the end the whole cavitation model by Singhal with small air content was tested, that means the following mathematical models were solved:

- A. flow of water without cavitation with air (2% and 0,05%),
- B. flow of water with cavitation without air,
- C. flow of water with cavitation and air.

2 MATHEMATICAL MODEL

2.1 Turbulent model of mixture

Two-equation $k-\varepsilon$ model is recommended for calculation of cavitation in literature [2], [4], [6] and [8]. The RNG $k-\varepsilon$ theory is advisable used for low-Reynolds number. This RNG $k-\varepsilon$ tur-

* Ing. Ph.D., Department of Hydromechanics and Hydraulic Equipment, Faculty of mechanical Engineering, VŠB-Technical University of Ostrava, tř. 17. listopadu 15, Ostrava, tel. (+420) 59 732 4385, e-mail jana.rautova@vsb.cz

** doc. RNDr. CSc., Department of Hydromechanics and Hydraulic Equipment, Faculty of mechanical Engineering, VŠB-Technical University of Ostrava, tř. 17. listopadu 15, Ostrava, tel. (+420) 59 732 3342, e-mail milada.kozubkova@vsb.cz

bulence model is derived from Navier-Stokes equations. Equations are defined by mean value (pressure, velocity) and are found in references [1], [2], [3], [4] and [6].

Water and vapour eventually air make multiphase mixture. For simulation multiphase flow is possible use Mixture model. This model is suitable, when the velocity of individual phase translation is different. Model enables solution with phase exchange. Volumetric fractions are defined for this occasion. In case of mixture multiphase flow of n phases the equations are defined for mixture.

The continuity equation applies to mean value of mixture:

$$\frac{\partial \rho_m}{\partial t} + \frac{\partial (\rho_m \bar{u}_{m,j})}{\partial x_j} = 0 \quad (1)$$

where:

ρ_m - is density,
 $\bar{u}_{m,j}$ - is the mass average velocity of the mixture,

$$\rho_m = \sum_{k=1}^n \alpha_k \rho_k, \quad \bar{u}_{m,j} = \frac{\sum_{k=1}^n \alpha_k \rho_k \bar{u}_{k,j}}{\rho_m} \quad (2)$$

where:

α_k - is the volume fraction of phase,
 k, n - is the number of phases.

The equation for momentum transfer can be obtained by summing the individual momentum equations for all phases:

$$\begin{aligned} \frac{\partial (\rho_m \bar{u}_{m,i})}{\partial t} + \frac{\partial (\rho_m \bar{u}_{m,i} \bar{u}_{m,j})}{\partial x_j} = & - \frac{\partial p}{\partial x_i} + \frac{\partial}{\partial x_j} \left(\mu_m \left(\frac{\partial \bar{u}_{m,i}}{\partial x_j} + \frac{\partial \bar{u}_{m,j}}{\partial x_i} \right) - \mu \delta_{ij} \frac{2}{3} \frac{\partial \bar{u}_{m,l}}{\partial x_l} \right) + \\ & + \rho_m f_i + \frac{\partial}{\partial x_j} \left(\sum_{k=1}^n \alpha_k \rho_k \bar{u}_{dr,k,j} \bar{u}_{dr,k,j} \right) \end{aligned} \quad (3)$$

where:

f_i - is the volume force (gravity),
 $\bar{u}_{dr,k,j}$ - is the slip velocity ($\bar{u}_{dr,k,j} = \bar{u}_{k,j} - \bar{u}_{m,j}$),
 μ_m - is the viscosity of the mixture defined by,

$$\mu_m = \sum_{k=1}^n \alpha_k \mu_k \quad (4)$$

Two-equation $k-\varepsilon$ model is complete equation for transport of turbulence kinetic energy k and velocity dissipation ε .

$$\frac{\partial (\rho_m k)}{\partial t} + \frac{\partial (\rho_m \bar{u}_{m,j} k)}{\partial x_j} = \frac{\partial}{\partial x_j} \left(\frac{\mu_t}{\sigma_k} \frac{\partial k}{\partial x_j} \right) + \underbrace{\mu_t \left(\frac{\partial \bar{u}_{m,j}}{\partial x_l} + \frac{\partial \bar{u}_{m,l}}{\partial x_j} \right) \frac{\partial \bar{u}_l}{\partial x_j}}_P \underbrace{g_j \frac{\mu_t}{\rho_m \sigma_h} \frac{\partial \rho_m}{\partial x_j}}_G - \rho_m \varepsilon \quad (5)$$

$$\frac{\partial (\rho_m \varepsilon)}{\partial t} + \frac{\partial (\rho_m \bar{u}_{m,j} \varepsilon)}{\partial x_j} = \frac{\partial}{\partial x_j} \left(\frac{\mu_t}{\sigma_\varepsilon} \frac{\partial \varepsilon}{\partial x_j} \right) + \rho_m c_{1\varepsilon} (P + c_{3\varepsilon} G) - \rho_m c_{2\varepsilon} \frac{\varepsilon^2}{k} \quad (6)$$

where P, G are terms of turbulence kinetic energy production due to tension and lift force.

2.2 Cavitation model

Cavitation model [7], [5] is used with multiphase mixture model defined above, two phases, water and vapour. Standard governing equations in the mixture model and the mixture turbulence model describe the flow and account for the effects of turbulence. A vapour transport equation governs the vapour mass fraction f_{vap} , given by:

$$\frac{\partial}{\partial t}(\rho f_{vap}) + \frac{\partial}{\partial x_j}(\rho f_{vap} \bar{u}_{vap j}) = \frac{\partial}{\partial x_j} \left(\gamma \frac{\partial f_{vap}}{\partial x_j} \right) + R_e - R_c \quad (7)$$

Values R_e and R_c are deduced from Rayleigh – Plesset equation and take under account limited size of the bubbles. These terms are influenced by value of immediate local static pressure p and are expressed as follows:

for $p < p_{sat}$

$$R_e = C_e \frac{v_{ch}}{\sigma} \rho_l \rho_{vap} \sqrt{\frac{2(p_{sat} - p)}{3\rho_l}} (1 - f_{vap}) \quad (8)$$

for $p > p_{sat}$

$$R_c = C_c \frac{v_{ch}}{\sigma} \rho_l \rho_l \sqrt{\frac{2(p - p_{sat})}{3\rho_l}} f_{vap} \quad (9)$$

where:

v_{ch} - is characteristic velocity, which is derived from local turbulent scale (e.g. $v_{ch} = \sqrt{k}$),

C_e, C_c - are empirical constants, standard $C_e = 0.02$, $C_c = 0.01$,

p_{sat} - is saturated vapour pressure at certain temperature,

ρ_l - is liquid density.

Influence of non-condensable air

The main phase – water – contains small amount of non-condensable air, which can have significant influence on cavitation region due to compressibility of air by low pressure. The calculation of the mixture density is modified as:

$$\frac{1}{\rho} = \frac{f_{vap}}{\rho_{vap}} + \frac{f_g}{\rho_g} + \frac{1 - f_{vap} - f_g}{\rho_l} \quad (10)$$

Non condensable gas density ρ_g is calculated as:

$$\rho_g = \frac{Mp}{RT} \quad (11)$$

Volume fractions of non condensable gas and liquid are modified as:

$$\alpha_g = f_g \frac{\rho}{\rho_g}, \quad \alpha_l = 1 - \alpha_{vap} - \alpha_g \quad (12)$$

where:

α_{vap} - is volume fraction of vapour,

α_g - is a volume fraction of gas.

Density of mixture can be defined too by:

$$\rho = \alpha_{vap} \rho_{vap} + \alpha_g \rho_g + (1 - \alpha_{vap} - \alpha_g) \rho_l \quad (13)$$

Finally, with the consideration of the non condensable gas effect, and also using \sqrt{k} to replace v_{ch} , we write:

$$R_e = C_e \frac{\sqrt{k}}{\sigma} \rho_l \rho_{vap} \sqrt{\frac{2(p_{sat} - p)}{3\rho_l}} (1 - f_{vap} - f_g) \quad (14)$$

$$R_c = C_c \frac{\sqrt{k}}{\sigma} \rho_l \rho_l \sqrt{\frac{2(p_{sat} - p)}{3\rho_l}} f_{vap} \quad (15)$$

3 NUMERICAL MODELLING

3.1 Description of Laval nozzle

The flow of water in divergent nozzle was solved. The geometry and input data were obtained from the experiment set up and installed at the Energy Institute - Victor Kaplan Dept. of Fluid Engineering, Faculty of Mechanical Engineering, Brno University of Technology, see [8].

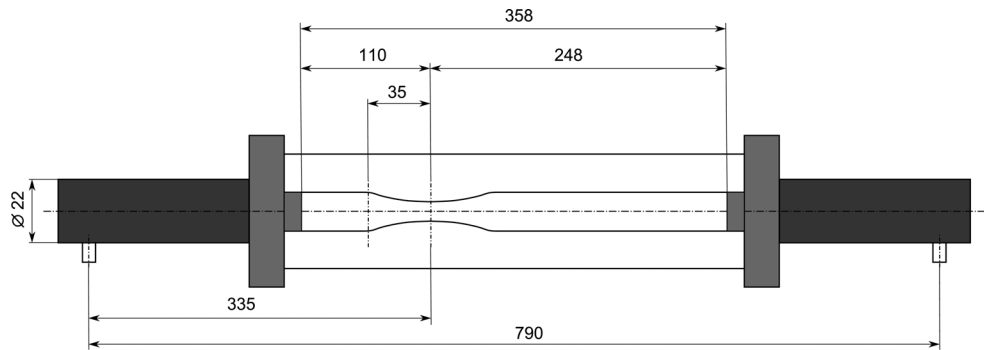


Fig. 1 Geometry of the nozzle

3.2 Boundary conditions

The same boundary conditions for all variants were defined, that means on the inlet the mass flow condition and at the outlet the pressure condition were chosen. The values of boundary conditions were measured on experimental equipment (VUT Brno), see Tab. 1.

The case was solved as axisymmetric region and time dependent case due to behaviour of pressure and velocity behind the pipe constriction.

Tab. 1 Boundary conditions

	A 2%	A 0,05%	B	C
inlet				
mass-flow of water [kg.s ⁻¹]	1,38753	1,38765	1,38756	1, 38756
mass-flow of vapour [kg.s ⁻¹]	-	-	0	0
mass-flow of air [kg.s ⁻¹]	3,44.10 ⁻⁵	8,45.10 ⁻⁷	-	-
outlet				
static pressure [Pa]	106623	106623	106623	106623
cavitation parameters				
saturated vapour pressure p_N [Pa]	-	-	2338 Pa	2338
surface tension coefficient σ [N.m ⁻¹]	-	-	0,717	0,717
non-condensable gas mass fraction f_A [1]	-	-	1,5.10 ⁻⁹	8,45.10 ⁻⁷

3.3 Physical properties

The flow of water is isothermal, so the physical properties were set as constant value at temperature 20°C (i. e. 293,15K). The air content in water is very important parameter. Two variants are calculated because the air content in water was not measured. Same experiments were executed without air and with 2% or 0,05% of air.

Tab. 2 Physical properties

	A 2%	A 0,05%	B	C
density [kg.m ⁻³]				
water	1000	1000	1000	1000
vapour	-	-	ideal-gas	ideal-gas
air	ideal-gas	ideal-gas	-	-
viscosity [Pa.s]				
water	0,000985	0,000985	0,000985	0,000985
vapour	-	-	8,854.10 ⁻⁶	8,854.10 ⁻⁶
air	1,789.10 ⁻⁵	1,789.10 ⁻⁵	-	-

4 RESULTS OF THE NUMERIC SOLUTION

The solution is time dependent, i.e. the velocity and pressure behind the constriction is periodically changing. It is obvious from Fig. 3. To compare the numerical results it is inevitable to stop the calculation, when the velocities at the inlet and outlet are the same (or the mass flows are the same). In Tab. 3 the mass flows at inlet and outlet are evaluated including the error.

Tab. 3 Mass flow at inlet and outlet and error

Mass Flow Rate [kg.s ⁻¹]	A 2%-1	A 2%-2	A 0,05%	B	C
inlet	1.3577585	1.3571259	1.3840908	1.387558	1.37786
outlet	-1.3193261	-1.3757968	-1.4194764	-3.131979	-1.2855129
difference	0.0384324	-0.0186709	-0.0353856	-1,744421	0.0923471
error	2,8306 %	1,3758 %	2,5566 %	125,72 %	6,7022 %

It is interesting, that the pressure drop along the pipe differs, if the calculation was stopped at velocity curve (4 m.s⁻¹) on ascend or descend part, see Fig. 2 and 3.

Variants A 2%-1 and A 2%-2

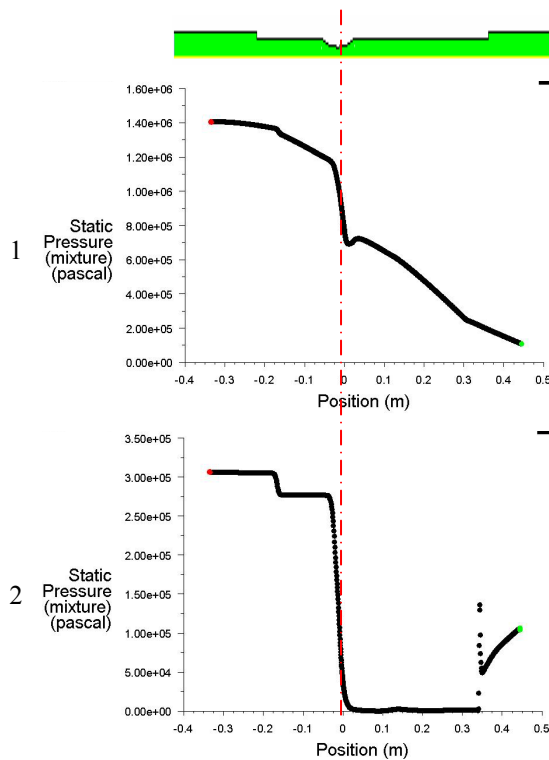


Fig. 2 Pressure distribution along the pipe

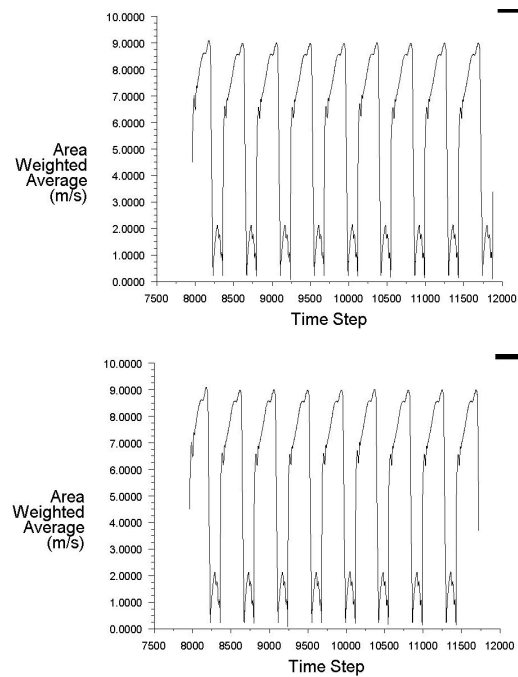


Fig. 3 Velocity curve vs. time at the outlet

The influence of the air amount is evaluated in Fig. 4. It is evident, that this parameter is very significant. The size of cavitation region obtained from experiment is compared here with size of air region gained from numerical solution.

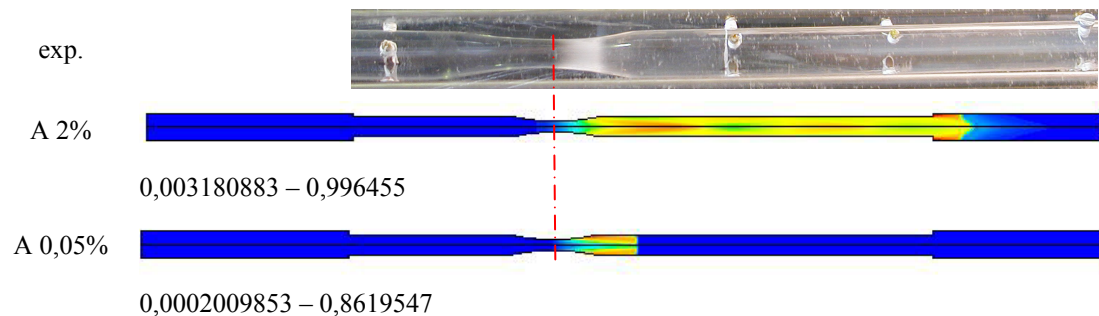


Fig. 4 Volume fraction of air

The pressure distribution along the pipe for all above defined variants is compared in Fig. 5. It is interesting, that the variants A 0,05% and C are comparable, only minimum of pressure in variant A 0,05% is equal 1Pa (limit value) and in variant C is equal 2328Pa (pressure of saturation).

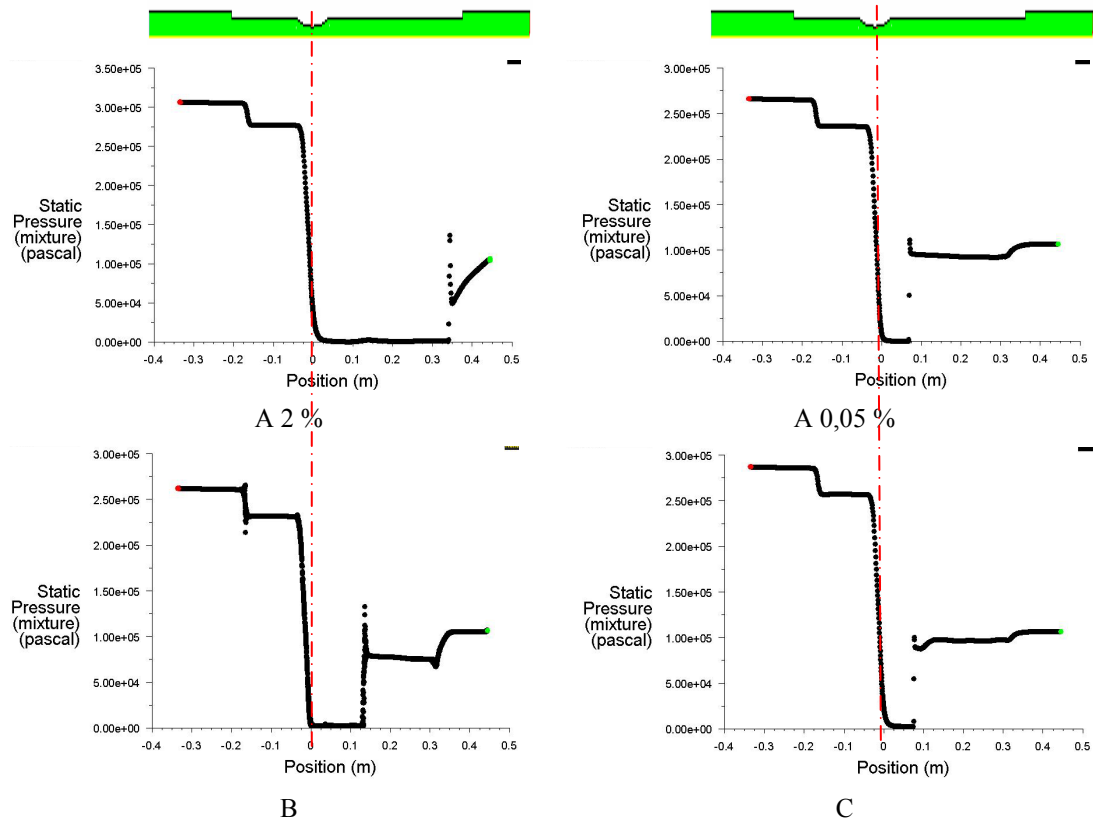


Fig. 5 Distribution of pressure for all variants

Variant B is not convergent. This can be observed in Fig. 6, where the velocity magnitudes for all variants vs. time are represented.

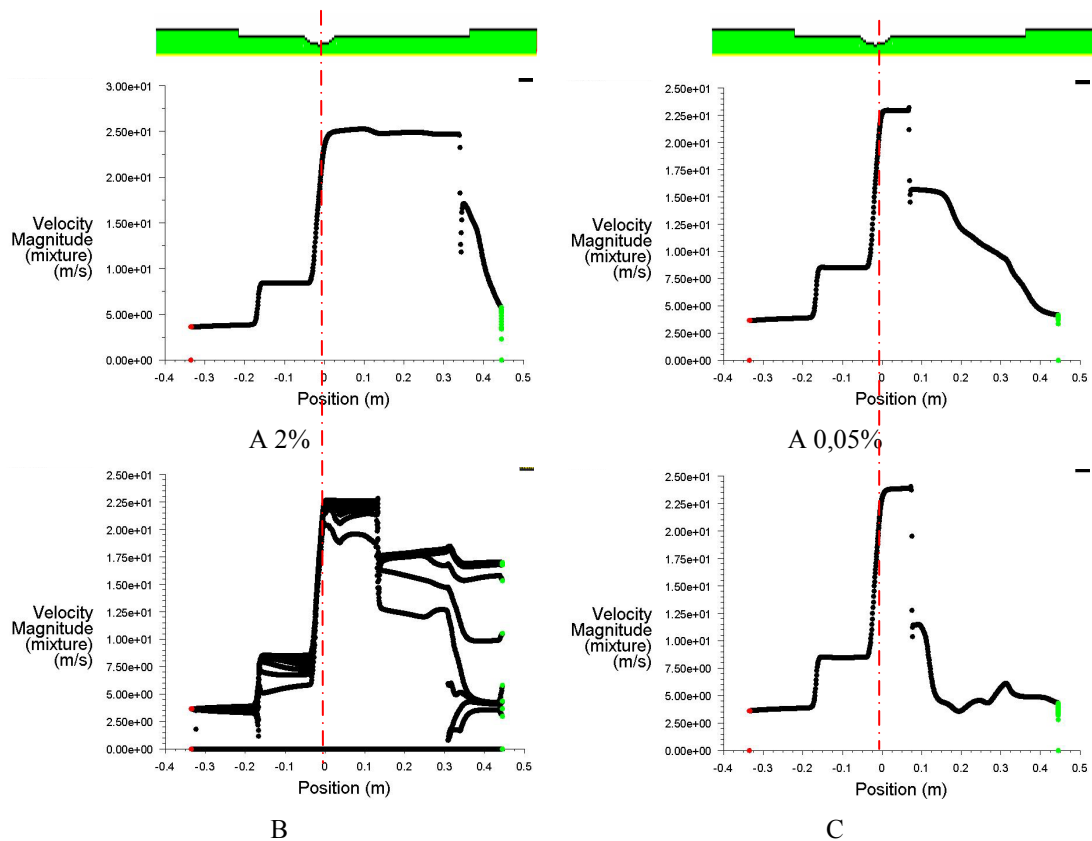


Fig. 6 Velocity magnitude distribution along the pipe

It is possible to find the air volume fraction in variant A 2% and A 0,05% (see Fig. 7 - vapour is not present in these mathematical models) and vapour volume fraction in variant B and C (see Fig. 8 - in variant B the air is not present and in variant C the air is present but it is not possible to evaluate it).

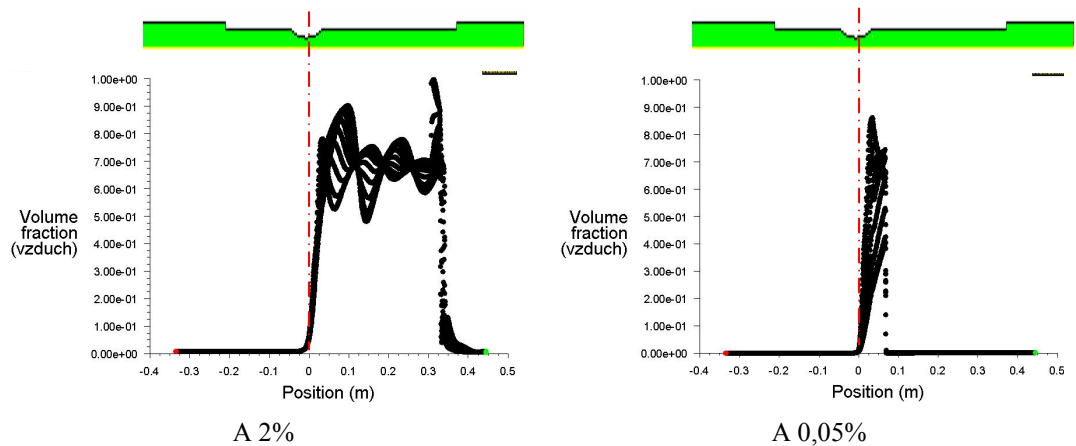


Fig. 7 Volume fraction of air

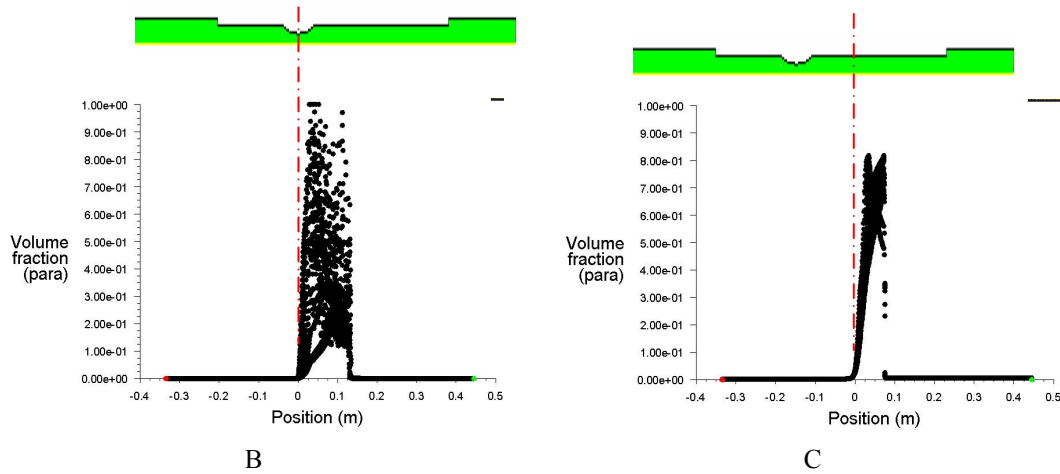


Fig 8 Volume fraction of vapour

The cavitation region from experiment is compared with numerical solution, see Fig. 9.

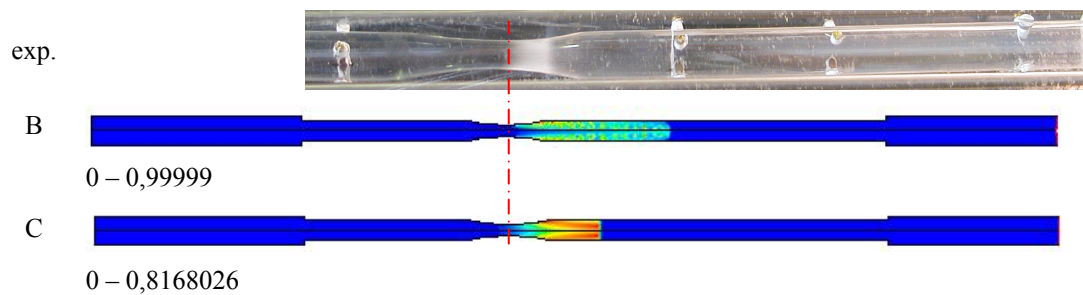


Fig. 9 Volume fraction of vapour

5 CONCLUSION

The paper presents, that the air content of air in the water is very important parameter that influences the convergence of numerical solution and primarily the dimension of cavitation region. But this parameter can not be measured readily and therefore the value was tested in numerical experiment. It seems that the physical experiment must be supplemented by equipment for air measurement in the future.

The curve of velocity magnitude vs. time at the outlet is significantly periodically dependent and it is possible to define the period or frequency of this phenomena. But to get the more accurate numerical solution, it is inevitable to prepare better physical experiment.

The cavitation region depending on rotating velocity inlet will be solved in the next research.

The work is supported by GA ČR č. 101/09/1715 Kavituující vírové struktury vyvolané rotací kapaliny

REFERENCES

- [1] KOZUBKOVÁ, M. *Matematické modely kavitace a hydraulického rázu*. 1.vydání, Ostrava: VŠB-TU Ostrava, 2009, 130 stran. ISBN 978-80-248-2043-9.
- [2] BOJKO, M.; KOVÁŘ, L.: Mathematical modelling of change technology the pure oxygen blowing on surface of liquid bath by additional oxygen fuel burner in metallurgical aggregates. In *Sborník vědeckých prací Vysoké školy báňské - Technické univerzity Ostrava, řada strojní, ročník LIV*, 2008. Ostrava : Vysoká škola báňská - Technická univerzita Ostrava, 2008, s. 13-20, ISBN 978-80-248-1891-7.
- [3] BLEJCHAR, T.; RÜDIGER, F.; HELDUSER, S. Schallentstehung in hydraulische Ventilen. *O+P: Organ des Forschungsfonds FLuidtechnik im VDMA*, číslo 4/2006, s. 187-190.
- [4] Ansys Fluent Inc. Fluent 12.16– User's guide. [Online]. c2009. Dostupné z: <URL:http://sp1.vsb.cz/DOC/Fluent_12.0.16/html/ug/main_pre.htm>.
- [5] SINGHAL, A.K., ATHAVALE, M. M., LI, H., JIANG, Y.: Mathematical Basis and Validation of the Full Cavitation Model. In *Journal of Fluids Engineering*, Vol. 124, 2002, p. 617-624.
- [6] KOZUBKOVÁ, M. Numerické modelování proudění – FLUENT I. [Online]. c2003. Ostrava: VŠB – TUO, 116 s, poslední revize 6.1.2005, Dostupné z: <URL:<http://www.338.vsb.cz/seznam.htm>>.
- [7] PLESSET, M., S. CHAMPMAN, R., B. Collapse of an initially spherical vapor cavity in the neighborhood of a solid boundary, *J. Fluid Mechanics*, 47, 1971, pp. 283-290.
- [8] RUDOLF, P.; HABÁN, V.; POCHYLÝ, F.; KOUTNÍK, J.; KRÜGER, K.: Collapse of cylindrical region and conditions for existence of elliptical vortex form of cavitating vortex rope. *Scientific Bulletin of the "Politehnica" University of Timisoara*, Vol.52, (2007), No.6, pp.109-118, ISSN 1224-6077, Politehnica University of Timisoara
- [9] LUKÁČ, P., ČARNOGURSKÁ, M., MIKOLAJ, D. Možnosti využitia vizualizačných metód pri skúmaní prúdových pomerov stlačiteľného média. In: *Nové trendy vývoja v oblasti obnoviteľných zdrojov energií po vstupe do Eurozóny: Zborník z 3. celoštátnej konferencie s medzinárodnou účasťou : 5.-7. november 2008, Hotel Permon, Podbanské, Vysoké Tatry, Slovakia. Košice : Steelcomp, 2008. s. 168-172. ISBN 978-80-232-0293-9.*
- [10] Gašparovic, P.: Použitie metód CFD pri návrhu súčastí (Use of CFD methods at design). In: *Zborník konferencie: Nové trendy v prevádzke výrobných technológií TU Košice so sídlom v Prešove, Nov. 2000. ISBN 8070996188.*

Reviewers:

Ing. Pavel Rudolf, Ph.D., VUT in Brno

Ing. Josef Foldyna, CSc., ÚG AVČR Ostrava